Disorder induced stripes in d-wave superconductors

Markus Schmid, Florian Loder, Arno P. Kampf, Thilo Kopp

PAPER • OPEN ACCESS

Disorder induced stripes in **d**-wave superconductors

View the article online for updates and enhancements.

Related content

- Modeling of superconducting stripe phases in high-Tc cuprates
  F Loder, S Graser, M Schmid et al.

- d-Wave superconductivity as a catalyst for antiferromagnetism in underdoped cuprates
  Markus Schmid, Brian M Andersen, Arno P Kampf et al.

- Stripe order and quasiparticle Nernst effect in cuprate superconductors
  Andreas Hackl and Matthias Vojta

Recent citations

- Fate of disorder-induced inhomogeneities in strongly correlated d-wave superconductors
  Debmalya Chakraborty and Amit Ghosal

New Journal of Physics

Disorder induced stripes in d-wave superconductors

Markus Schmid[1], **Florian Loder**[1,2,3]**, Arno P Kampf**[1]
and Thilo Kopp[2]

[1] Center for Electronic Correlations and Magnetism, Theoretical Physics III, Institute of Physics, University of Augsburg, D-86135 Augsburg, Germany
[2] Center for Electronic Correlations and Magnetism, Experimental Physics VI, Institute of Physics, University of Augsburg, D-86135 Augsburg, Germany
E-mail: florian.loder@physik.uni-augsburg.de

Abstract. Stripe phases are observed experimentally in several copper-based high-T_c superconductors near 1/8 hole doping. However, the specific characteristics may vary depending on the degree of dopant disorder and the presence or absence of a low-temperature tetragonal phase. On the basis of a Hartree–Fock decoupling scheme for the t–J model, we discuss the diverse behavior of stripe phases. In particular, the effect of inhomogeneities is investigated in two distinctly different parameter regimes which are characterized by the strength of the interaction. We observe that small concentrations of impurities or vortices pin the unidirectional density waves, and dopant disorder is capable of stabilizing a stripe phase in parameter regimes where homogeneous phases are typically favored in clean systems. The momentum-space results exhibit universal features for all coexisting density-wave solutions, nearly unchanged even in strongly disordered systems. These coexisting solutions feature generically a full energy gap and a particle–hole asymmetry in the density of states.

[3] Author to whom any correspondence should be addressed.

IOP Institute of Physics **Φ** DEUTSCHE PHYSIKALISCHE GESELLSCHAFT

Contents

1. Introduction

Stripe ordering phenomena on the nanoscale seem to be an inherent consequence of electronic correlations in high-T_c superconducting (SC) materials. They are most prominently close to $x = 1/8$ hole doping [1–4], but they were also identified within a broader doping range in the pseudo-gap regime [5–7]. However, the nature of the stripe order varies significantly for different cuprate materials.

Unidirectional charge waves (CDW) and spin-density waves (SDW) have been detected in many cuprates by neutron scattering and x-ray experiments [1, 3, 4, 8–17]. However, the details are strongly material dependent. Neutron-scattering experiments on $La_{2-x-y}Nd_ySr_xCuO_4$ (LNSCO) at $x = 1/8$ [1, 12–14] revealed static antiferromagnetic (AF) SDW order with a period of eight lattice constants and a concomitant charge-density wave with half this period. A similar spin structure was found in $La_{2-x}Ba_xCuO_4$ (LBCO) [3, 9, 10, 15], in $La_{2-x}Ba_ySr_{x-y}CuO_4$ (LBSCO) (with $y = 0.075$) [4] and in $La_{2-x-y}Eu_ySr_xCuO_4$ [16, 17], where SDW and CDW coexist at and near $x = 1/8$. A common feature of these cuprates is an anisotropic low-temperature tetragonal (LTT) phase and, in addition, a strong dopant disorder; both the LTT structure and dopant disorder are supposed to pin stripes. However, not all cuprates exhibit an LTT phase or dopant disorder. While every chemical doping of the cuprate parent compounds introduces disorder, its impact on the SC properties depends decisively on the distance between the CuO_2 planes and dopants. In $La_{2-x}Sr_xCuO_4$ (LSCO) dopants are randomly positioned close to the CuO_2 planes generating effective disordered impurity potentials to the in-plane electrons. In contrast, oxygen dopants order in CuO chains in $YBa_2Cu_3O_{7-\delta}$ (YBCO) that are separated from the CuO_2 planes by a BaO plane, and they are roughly at twice the distance from the CuO_2 planes than Sr is in LSCO. Hence, YBCO is minimally affected by the dopants' impurity potentials and is therefore considered as the cleanest material in the cuprate family. In pure LSCO, which exhibits no LTT phase, spin stripes have been detected below T_c but no CDW order [18, 19]. Although no static stripes have so far been reported for YBCO, electron-nematic order is inferred from anisotropies [20] found in neutron scattering [21] and thermoelectric transport [22] measurements. In addition, incommensurate spin fluctuations are detected in SC YBCO, and a static CDW appears in the presence of an external magnetic field [23, 24].

The different behavior of YBCO may arise from both the absence of dopant disorder and the LTT structure. Stripe phenomena in cuprates must therefore be considered strongly material specific. Here we present a comprehensive analysis of their delicate response to the presence of disorder.

In the last few years, the theoretical understanding of stripe formation in cuprates has advanced. Early on neutron-scattering data on LNSCO at hole doping $x = 1/8$ [1] suggested the formation of a spin-ladder structure in the CuO_2 planes. This structure is built from half-filled, three-legged spin ladders, separated by quarter-filled chains. The AF spin structure changes sign from one ladder to the next, resulting in a wavelength of eight lattice constants. This same spin structure was later detected also in LBCO [8]. Indeed, theoretical models based on coupled spin-ladders describe [25, 26] with some success inelastic neutron-scattering data on LBCO [3]. Already before the experimental discovery of stripes, Zaanen and Gunnarsson [24] and Machida [27] predicted the formation of spin stripes in doped AFs from mean-field analyses of the Hubbard model. The spin stripes suggested by Tranquada and co-workers were found also in various numerical calculations using the Hubbard model [28], the $t–J$ model [29–36] or the spin–fermion model [37], and their existence is by now well established.

A more delicate problem is understanding the coexistence of or competition between spin- and charge-stripe order and superconductivity. It has been known for some time that in a d-wave superconductor (dSC) with an on-site repulsion U (to which we refer as the 'U-model'), antiferromagnetism nucleates around impurity sites [38, 39]. Depending on the spatial configuration of the impurities, connected AF domains may form building networks of quasi-one-dimensional (1D) AF lines [39, 40]. On the other hand, in homogeneous systems, the above described spin-ladder state was found to coexist with a striped form of d-wave superconductivity within a mean-field treatment of the $t–J$ model and variants of it [41–44]. This SC state is modulated in space with the same period as the spin structure; its SC order parameter is minimal in the center of the AF spin ladder and maximal in between the spin stripes. Striped superconductivity in this context corresponds to a unidirectional pair-density wave (PDW) state [45, 46]. Notably, this PDW oscillates with twice the wavelength of the accompanying CDW, which is caused by periodic zero crossings of the SC order parameter. Below we discuss and contrast the PDW state with the periodically modulated dSC (mdSC), which lacks a sign change and thus oscillates with the same wavelength as the CDW.

The emerging static spin order in these models is typically rather robust and remains unchanged in a wide range of parameters and hole density. This is in contrast to the spin stripes found in the cuprates, the wavelength of which seems to shrink continuously with increasing hole doping. One might therefore ask whether the stripe phenomena in cuprates are not better described by the glassy stripe structures emerging from the disordered U-model. Indeed, it was shown in [44] that the U-model is actually the weak-coupling limit of the mean-field decoupled $t–J$ model. The U-model is therefore expected to exhibit the same stripe order as the $t–J$ model, and it is the disorder (as induced, e.g. by dopant atoms) that qualitatively changes the nature of the spin-stripe structures.

In this paper, we discuss the impact of inhomogeneities on striped superconductors within the U- and the V-model. Additionally, the effect of magnetic vortices is studied, which proves to have a similar impact on the stripe formation as isolated strong impurities. In section 2, we introduce the U-model as the weak-coupling limit of the mean-field decoupled $t–J$ model and derive also the strong-coupling limit, to which we refer to as the 'V-model'. By comparing the two limits, we conclude that only the U-model shows the large susceptibility to disorder

and the doping dependence of the stripe structure observed experimentally. The cuprates are nevertheless estimated to be placed in between the two limits. Some cuprate materials show characteristics that are qualitatively explained by the V-model, whereas others come closer to the physics of the U-model. In this regime, the strengths of SC and AF correlations are in balance and material-specific details matter [44]. By relating our theoretical results with the experimental observations, we conclude in section 4 that disorder is essential for understanding the nature of the stripe phases in cuprate superconductors.

2. Hamiltonian

We follow the general idea that the one-band Hubbard model describes well the low-energy physics of the CuO_2 planes of the cuprates, including antiferromagnetism and superconductivity [47]. At strong coupling, a unitary transformation maps the Hubbard model onto the $t-J$ model with an AF exchange coupling $J = 4t^2/U$ [48]. The non-local interaction in the $t-J$ model accounts for both superconductivity and antiferromagnetism already on the mean-field level [49–53]. Here we use an ansatz introduced by Kagan and Rice [52], in which the projection to exclude doubly occupied sites is replaced by an on-site repulsion term $U/2 \sum_{i,\sigma} n_{i,\sigma} n_{i,-\sigma}$, leading back to the original $t-J$ model in the limit $U \to \infty$. On mean-field level, this ansatz is equivalent to the fully decoupled Bardeen–Cooper–Schrieffer (BCS) Hamiltonian $\mathcal{H}_{UV}$ with attractive nearest-neighbor interaction of strength V and an on-site repulsion of strength U, if V is identified with J [44]. We employ this model on a square lattice including randomly positioned on-site impurity potentials V_i^{imp} and a perpendicular orbital magnetic field. Specifically, the model Hamiltonian reads

$$\mathcal{H}_{UV} = -\sum_{ij\sigma} t_{ij} \mathrm{e}^{\mathrm{i}\varphi_{ij}} c_{i,\sigma}^{\dagger} c_{j,\sigma} - \frac{V}{2} \sum_{\langle ij \rangle,\sigma} c_{i,\sigma}^{\dagger} c_{j,-\sigma}^{\dagger} c_{j,-\sigma} c_{i,\sigma} + \frac{U}{2} \sum_{i,\sigma} n_{i,\sigma} n_{i,-\sigma} + \sum_{i,\sigma} \left(V_i^{\mathrm{imp}} - \mu \right) c_{i,\sigma}^{\dagger} c_{i,\sigma},$$

(1)

where $c_{i,\sigma}^{\dagger}$ creates an electron on-site i with spin $\sigma = \uparrow, \downarrow$ and $n_{i,\sigma} = c_{i,\sigma}^{\dagger} c_{i,\sigma}$. The hopping matrix elements between nearest and next-nearest neighbor sites are denoted by $t_{ij} = t$ and $t' = -0.4\,t$, respectively. An electron moving in the external magnetic field from site j to i acquires the Peierls phase $\varphi_{ij} = (\pi/\Phi_0) \int_{\mathbf{r}_j}^{\mathbf{r}_i} \mathbf{A}(\mathbf{r}) \cdot \mathrm{d}\mathbf{r}$, where $\Phi_0 = hc/2e$ and $\mathbf{A}(\mathbf{r}) = (0, xB)$ is the vector potential in the Landau gauge. The attractive nearest-neighbor interaction is parameterized by $V > 0$ and the chemical potential μ is adjusted to fix the electron density $n = \sum_i \langle n_i \rangle / N = 1 - x$, where x is the hole concentration. The impurity potentials V_i^{imp} are used to simulate the effect of either a single impurity or of the disorder introduced by the dopant atoms, the case in which the density of impurities is equal to the hole concentration x.

The Hamiltonian $\mathcal{H}_{UV}$ approaches the physics of the Hubbard model for $U \to \infty$. Nevertheless, a thorough mean-field analysis of its ground-state solutions showed that, at finite values of U, it is well suited to describe the combined emergence of superconductivity and antiferromagnetism as observed in the cuprates [44]. A mean-field decoupling of the interaction $-V/2 \sum_{\langle ij \rangle,\sigma} c_{i,\sigma}^{\dagger} c_{j,-\sigma}^{\dagger} c_{j,-\sigma} c_{i,\sigma}$, leads to the standard term for BCS-type superconductivity, and additionally to an AF interaction term of the form $-V \sum_{\langle ij \rangle,\sigma} \langle n_{i,\sigma} \rangle n_{j,-\sigma}$. At half-filling, the ground state of this model is an AF Mott insulator, while far enough from half-filling, it is a dSC. While both situations are captured within a mean-field decoupling scheme, this approximation is not considered adequate to describe the correlation physics of the doped Mott insulator close

to but slightly below half-filling (e.g. at $x = 1/8$). In [44], two special situations were identified where a mean-field decoupling is nonetheless meaningful: (i) if the interaction V is small ($V \ll t$), its pairing component is dominant and antiferromagnetism acts only as a perturbation to the SC ground state. In this regime, the term $-V \sum_{\langle ij \rangle, \sigma} \langle n_{i,\sigma} \rangle n_{j,-\sigma}$ is of minor relevance, and antiferromagnetism is controlled by U. Thus we denote this limit the U-model. (ii) On the other hand, if V is large ($V \gtrsim t$), the system separates locally into half-filled AF stripes separated by hole-rich, metallic (or SC, respectively) regions. Since V in this case is sufficient to almost maximally spin polarize the AF sites, the term $(U/2) \sum_{i\sigma} n_{i,\sigma} n_{i,-\sigma}$ is negligible. Therefore, we call this limit the V-model. Since antiferromagnetism appears here only in half-filled, spatially separated regions, a mean-field decoupling is feasible. Physically meaningful results can therefore be obtained from our model in the weak- and strong-coupling limits, while the intermediate-coupling regime is not accessible in a mean-field calculation.

2.1. U-model

As discussed above, the interaction $-V/2 \sum_{\langle ij \rangle, \sigma} c_{i\sigma}^{\dagger} c_{j-\sigma}^{\dagger} c_{j-\sigma} c_{i\sigma}$ is not important for magnetism in the limit $V \ll t$, but leads to the standard BCS expression for the SC order parameter. Thus, the Hartree–Fock decoupling of $\mathcal{H}_{UV}$ can be restricted to the U-model:

$$\mathcal{H}_U = -\sum_{ij\sigma} t_{ij}\, e^{i\varphi_{ij}}\, c_{i\sigma}^{\dagger} c_{j\sigma} - \mu \sum_{i\sigma} c_{i\sigma}^{\dagger} c_{i\sigma} + \sum_{\langle ij \rangle} \left(\Delta_{ij} c_{i\uparrow}^{\dagger} c_{j\downarrow}^{\dagger} + \text{h.c.} \right) + \frac{U}{2} \sum_i \left(\langle n_i \rangle n_i - \langle \sigma_i^z \rangle \sigma_i^z \right)$$
$$+ \sum_{i\sigma} V_i^{\text{imp}} c_{i\sigma}^{\dagger} c_{i\sigma}, \tag{2}$$

where $\sigma_i^z = (n_{i\uparrow} - n_{i\downarrow})/2$. In the following, we will focus mainly on hole densities at and near $x = 1/8$. The non-local pairing amplitude is defined as

$$\Delta_{ij} = -V \langle c_{j\downarrow} c_{i\uparrow} \rangle. \tag{3}$$

We do not include spin-flip terms of the form $\langle c_{i\uparrow}^{\dagger} c_{i\downarrow} \rangle c_{i\downarrow}^{\dagger} c_{i\uparrow}$, because they do not conserve the spin as the original Hamiltonian (1) does. Furthermore, the inclusion of a finite spin-flip term in the factorization acts only as a rotation of the spin-quantization axis, but contributes neither to superconductivity nor to antiferromagnetism. The U-model has been the starting point for numerous investigations on disorder- [38, 39, 54–57] and field-induced antiferromagnetism [39, 57–59]. Within a certain hole-doping regime and most prominently around $x = 1/8$, the ground state exhibits AF spin-stripes, if U exceeds the critical value U_c.

All fields, i.e. Δ_{ij}, the local electron density $\langle n_i \rangle$ and the local magnetization $\langle \sigma_i^z \rangle$ are calculated self-consistently from the solutions of the associated Bogoliubov–de Gennes (BdG) equations. A detailed derivation of the BdG equations is presented in [39, 59]. The d-wave order parameter on a lattice site i is defined as

$$\Delta_i^d = \tfrac{1}{4} \left(\Delta_{i,i+\hat{x}}^d + \Delta_{i,i-\hat{x}}^d - \Delta_{i,i+\hat{y}}^d - \Delta_{i,i-\hat{y}}^d \right), \tag{4}$$

where $\Delta_{i,j}^d = \Delta_{ij}\, e^{-i\varphi_{ij}}$. In order to describe a possibly appearing modulation of the SC order parameter, as in the PDW state [43, 44, 46, 60, 61], we subdivide the pairing order parameter into three contributions [46, 61]

$$\Delta_i^d = \Delta_0 + \Delta_{\mathbf{q}}\, e^{i\mathbf{q} \cdot \mathbf{r}_i} + \Delta_{-\mathbf{q}}\, e^{-i\mathbf{q} \cdot \mathbf{r}_i}, \tag{5}$$

where the wave vector $\mathbf{q}$ parameterizes the modulation of the pairing amplitude and reflects a finite center-of-mass momentum $\hbar\mathbf{q}$ of the electron pairs. Δ_0 accounts for a homogeneous component of the order parameter. Two distinct types of SC states are possible solutions for $\mathcal{H}_U$: If $\Delta_0 = 0$, the SC order parameter shows a stripe pattern modulated with wave vector $\mathbf{q}$, where the SC stripes are separated by channels of zero pairing amplitude across which the SC order parameter changes sign. If the absolute values of $|\Delta_{\mathbf{q}}|$ and $|\Delta_{-\mathbf{q}}|$ are smaller than the homogeneous component $|\Delta_0|$, Δ_i^d is always finite and modulated with wave vector $2\mathbf{q}$. Although the 'pure' PDW with $\Delta_0 = 0$ was phenomenologically suggested to be the ground state of striped high-T_c superconductors [45], all calculations of mean-field type so far led to ground states with dominating uniform component Δ_0, cf [42, 44].

2.2. V-model

For large attractive interactions $V \sim t$, the Hartree–Fock decoupled Hamiltonian of equation (1) is effectively described by the V-model Hamiltonian

$$H_V = -\sum_{i,j,\sigma} t_{ij} \mathrm{e}^{\mathrm{i}\varphi_{ij}} c_{i\sigma}^\dagger c_{j\sigma} - \mu \sum_{i,\sigma} c_{i\sigma}^\dagger c_{i\sigma} + \sum_{\langle i,j \rangle} \left(\Delta_{ij} c_{i\uparrow}^\dagger c_{j\downarrow}^\dagger + \mathrm{h.c.} \right) - V \sum_{\langle i,j \rangle,\sigma} \langle n_{i\sigma} \rangle c_{j-\sigma}^\dagger c_{j-\sigma}$$
$$+ \sum_{i,\sigma} V_i^{\mathrm{imp}} c_{i\sigma}^\dagger c_{i\sigma}, \tag{6}$$

where Δ_{ij} is defined as in equation (3). The term $\langle n_{i\sigma} \rangle c_{j-\sigma}^\dagger c_{j-\sigma}$ is responsible for antiferromagnetism; it is controlled by the same interaction parameter V as the SC order parameter. Since in this limit AF correlations are strong enough to separate the system locally into AF regions close to half-filling and into hole-rich regions far from half-filling, the U-term contributes little. Even for values of U as large as the bandwidth, the U-term does not have a qualitative effect on the ground-state solutions [44].

For hole doping around $x = 1/8$, the solutions of the BdG equations for H_V in the impurity-free case are very similar to those of the U-model [44]. The main difference is the hierarchy of SC and AF order: in the U-model, two-dimensional superconductivity is the dominant order, i.e. the SC energy gap dominates over the AF gap, up to a certain value of U, above which the AF gap takes over and superconductivity is destroyed. In the V-model the hierarchy is reversed. Antiferromagnetism appears only if V is sufficiently large to induce an AF energy gap, which dominates over the SC gap. Superconductivity is thereby destroyed within the AF stripes and the regions where superconductivity persists are spatially separated into uncorrelated, quasi-1D filaments. Therefore, the phase relation between them is not fixed and the 'pure' PDW state is degenerate to a solution with finite Δ_0. Because of the 1D character of the solutions of the V-model, they barely adjust to impurities in comparison with the solutions of the U-model. This characteristic difference is discussed in section 3.2.

2.3. Momentum-space quantities

For a thorough analysis of our results we also discuss the following momentum-space quantities. With the Fourier transform of the factorized square of the magnetization

$$S(\mathbf{q}) = \left| \frac{1}{N} \sum_i \langle \sigma_i^z \rangle \, \mathrm{e}^{-\mathrm{i}\mathbf{q}\cdot\mathbf{r}_i} \right|^2, \tag{7}$$

we approximate the magnetic structure factor. In addition, we discuss the absolute squares of the Fourier transformed (FT) d-wave order parameter

$$|\Delta(\mathbf{q})|^2 = \left| \frac{1}{N} \sum_i \Delta_i^{\mathrm{d}} \, \mathrm{e}^{-\mathrm{i}\mathbf{q}\cdot\mathbf{r}_i} \right|^2 \tag{8}$$

and the deviation from the average electron density n

$$|n(\mathbf{q})|^2 = \left| \frac{1}{N} \sum_i \left(\langle n_i \rangle - n \right) \mathrm{e}^{-\mathrm{i}\mathbf{q}\cdot\mathbf{r}_i} \right|^2. \tag{9}$$

In the strong disorder limit, the suppression of the electron density at the random impurity sites dominates the charge distribution even for small impurity potentials. Coherent charge oscillations with small amplitudes are therefore barely visible in the Fourier transform $n(\mathbf{q})$. Since we are especially interested in these coherent charge modulations, we exclude the impurity sites in the presence of strong disorder from the sum over sites in the Fourier transformation.

The momentum distribution is given by

$$n(\mathbf{k}) = \sum_\sigma \langle c_{\mathbf{k}\sigma}^\dagger c_{\mathbf{k}\sigma} \rangle, \tag{10}$$

where the fermionic operators $c_{\mathbf{k}\sigma}$ are the Fourier transform of the real-space operators $c_{i\sigma}$. The spectral density at the Fermi energy $A(\mathbf{k}) \equiv A(\mathbf{k}, \omega = 0)$ is determined from the imaginary part of the retarded Green function

$$A(\mathbf{k}, \omega) = -\frac{1}{\pi} \sum_\sigma \mathrm{Im}\langle\langle c_{\mathbf{k}\sigma}; c_{\mathbf{k}\sigma} \rangle\rangle_\omega^{\mathrm{ret}}. \tag{11}$$

$A(\mathbf{k})$ allows for the determination of partially reconstructed Fermi surfaces which are characteristic for inhomogeneous superconductors. Homogeneous dSCs exhibit a finite gap away from the nodes on the Brillouin zone diagonals. $n(\mathbf{k})$ is therefore continuous everywhere except across the nodes. However, stripe formation leads to a reconstruction of the Fermi surface attributed to finite pairing momentum. In this case, the pair density $P(\mathbf{k})$ (equation (12)) is readjusted and, as a result, the SC energy gap no longer covers all sectors of the underlying Fermi surface. Impurities, on the other hand, induce bound states within the SC gap, leading to a redistribution of spectral weight into the gap which can be observed in $A(\mathbf{k})$. In this process, the transition from partially filled to empty states in $n(\mathbf{k})$ narrows, implicating a partial reconstruction of the Fermi surface.

The momentum distribution of the pair density $P(\mathbf{k})$ is defined as [44, 62]

$$P^2(\mathbf{k}) = \sum_\mathbf{q} \left| \langle c_{-\mathbf{k}+\mathbf{q}\downarrow} c_{\mathbf{k}\uparrow} \rangle \right|^2. \tag{12}$$

It measures the average correlation of the two occupied electron states $|\mathbf{k}, \uparrow\rangle$ and $|-\mathbf{k}-\mathbf{q}, \downarrow\rangle$ and thereby the parts of the Brillouin zone where electron pairing occurs. Eventually, we discuss the information contained in

$$\rho_S(\mathbf{k}) = \frac{1}{2} \sum_{\mathbf{q}\sigma} \langle \sigma\, c_{\mathbf{k}+\mathbf{q}\sigma}^\dagger c_{\mathbf{k}\sigma} \rangle \tag{13}$$

on the spin state. This quantity is maximal in those parts of the Brillouin zone where antiferromagnetism dominates. Thus, the competition between superconductivity and antiferromagnetism can be analyzed by comparing $P(\mathbf{k})$ and $\rho_S(\mathbf{k})$.

3. Results

3.1. U-model

The Hamiltonian (2) gives rise to unidirectional stripes [44, 54, 59, 63, 64] or checkerboard patterns [65, 66], which have been identified in the real-space quantities of clean dSCs above a critical on-site repulsion U_c. The role of disorder for the competition between stripe and checkerboard CDW order in the non-SC state was analyzed in [67, 68]. For a clean ($V^{imp} = 0$) dSC, the free energy of stripe solutions is typically close to the homogeneous dSC solutions. Depending sensitively on the initial conditions of the self-consistent BdG calculations, we find either stripes or homogeneous AF order both coexisting with superconductivity. In clean systems, regular stripe solutions emerge only if the self-consistency loop is started from a striped initial state. However, in the presence of perturbations, such as impurities or vortices, or by a rectangular lattice geometry, stripes are pinned and the stripe solutions become robust against the changes of the initial conditions. This relates to the notion that in the unperturbed superconductor fluctuating stripes are present, which become static by the pinning to defects [54, 59, 63].

In the U-model below a critical pairing interaction, an emerging stripe state exhibits a dominant uniform component of the SC order parameter, i.e. $\Delta_0 \neq 0$ in equation (5), in addition to the finite-momentum pairing amplitudes. In this case, the SC order parameter Δ_i^d does not feature a sign change and we call this state an mdSC. In [69], it was shown within a momentum-space formulation that a translation-invariant Hamiltonian in zero magnetic field can nevertheless support a 'pure' PDW ground state with $\Delta_0 = 0$ for a similar set of parameters but with a stronger pairing interaction $V \gtrsim 2.2\,t$. There, an analytic approximation to Gor'kov's equations was considered. Solutions of this kind are also found in the impurity-free real-space model used here, although the PDW solution converges into a *local* energy minimum and is slightly higher in energy than the mdSC solution. Stripe solutions are indeed observed in a broad hole-doping range. In the strong disorder limit, however, we find stripe states only close to $x = 1/8$.

3.1.1. Impurity-free stripe solutions. Choosing sinus-shaped initial values with a wavelength of $8a$ for the self-consistent fields Δ_{ij} and $m_i = \langle \sigma_i^z \rangle$, the impurity-free system ($V^{imp} = 0$) exhibits horizontal (or vertical) stripes in the real-space quantities over a wide hole-doping range. In figure 1, the order parameter, the electron density and the staggered magnetization are shown for $x = 1/8$. Obviously, a CDW, a SDW and a modulated pair-density (mdSC) ($\Delta_q \neq 0$) coexist in such a striped superconductor. The SC order parameter is *finite* everywhere, modulated only with an amplitude of a few per cent of the average order parameter $\overline{\Delta}_i^d$. The CDW oscillates around the average density n with an amplitude of only 1%. The staggered magnetization exhibits the strongest modulation with an amplitude of about $0.5\,\mu_B$ including a periodic sign change in the vertical direction corresponding to anti-phase domain walls between the antiferromagnetically ordered stripes. This solution is the ground state of the U-model for the chosen parameters and initial conditions.

The periodic modulation of the magnetization in the vertical direction translates into two distinct peaks in the magnetic structure factor at the wave vectors $\mathbf{q}_m = (2\pi/a)(1/2, 1/2 \pm \epsilon)$ with $\epsilon = 1/8$. These magnetic ordering wave vectors $\mathbf{q}_m$ correspond to an SDW with period $8a$ perpendicular to the stripes as is also obvious from the real-space pattern of the staggered magnetization in figure 1(c).
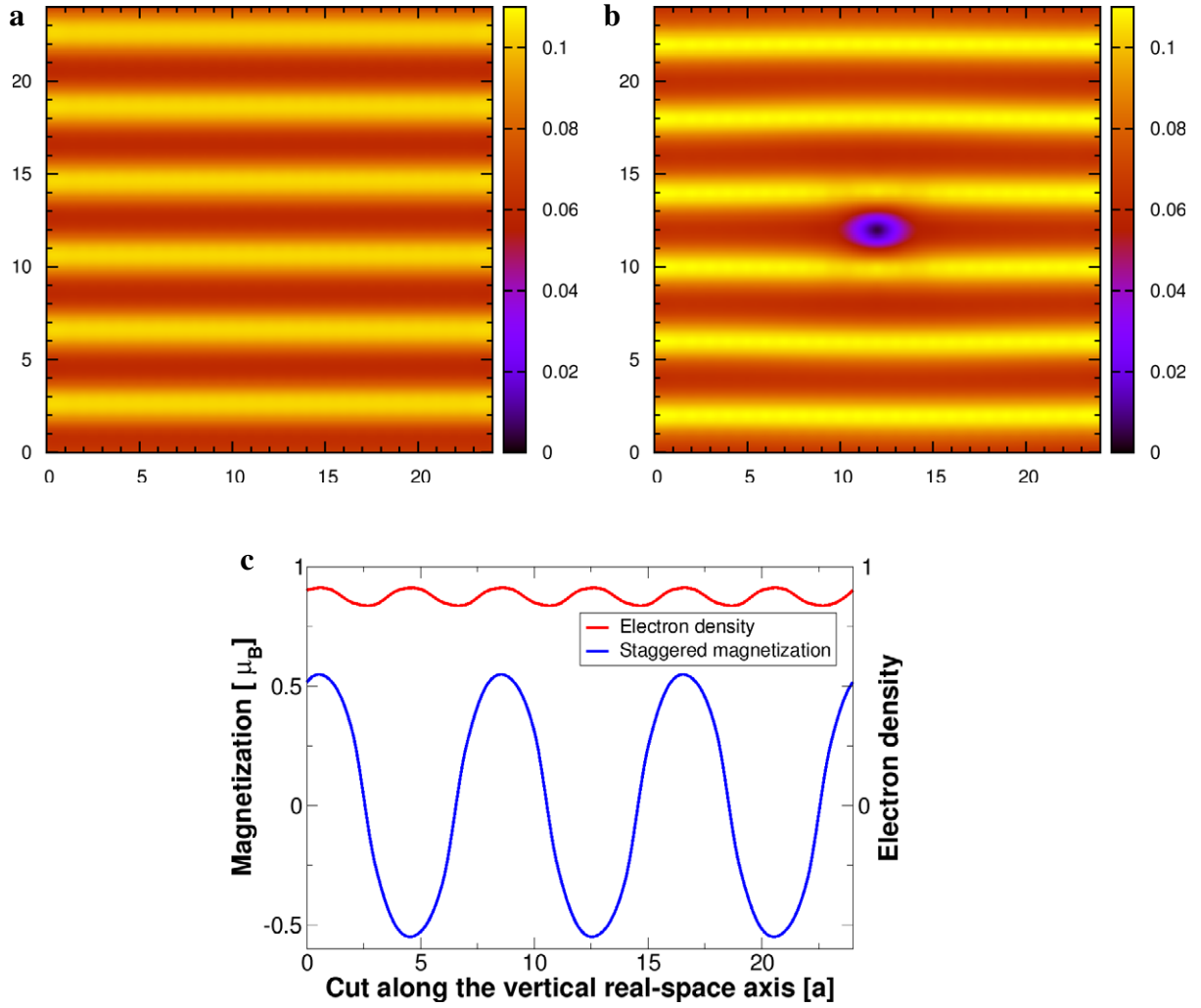
Figure 1. Density modulations of a d-wave superconductor. SC order parameter Δ_i^d for an (a) impurity-free and an (b) impurity-pinned ($V^{\mathrm{imp}} = 10t$) stripe solutions. (c) Vertical cuts of the electron density and the staggered magnetization in the impurity-free case ($V^{\mathrm{imp}} = 0$). These calculations were performed on a $24a \times 24a$ lattice where a is the lattice constant. Parameters were fixed to $T = 0.025\,t$, $t' = -0.4\,t$, $V = 1.5\,t$, $x = 1/8$, $U = 3.3t$.

The concomitantly emerging CDW (figure 1(c)) and mdSC (figure 1(a)) modulate with half the wavelength compared to the fluctuating SDW. Their Fourier transforms peak at $\mathbf{q}_{c/p} = 2\pi/a\,(0, \pm\delta)$ with $\delta = 1/4$ indicating a vertical oscillation with wavelength $\lambda_{\mathrm{CDW/mdSC}} = 4a$. The period doubling of the SDW results from the π-phase shift that the spin order experiences between neighboring charge stripes. In contrast to the PDW, which contains *no* uniform $\mathbf{q} = \mathbf{0}$ pairing component, the SC order parameter is here always of equal sign. These wavelengths stay fixed in a hole doping range from $x = 0.1$ to 0.15. For $x > 1/8$, the additional holes collected in the already present stripes deepens the hole-rich channels, thus increasing the oscillation amplitude of the CDW.
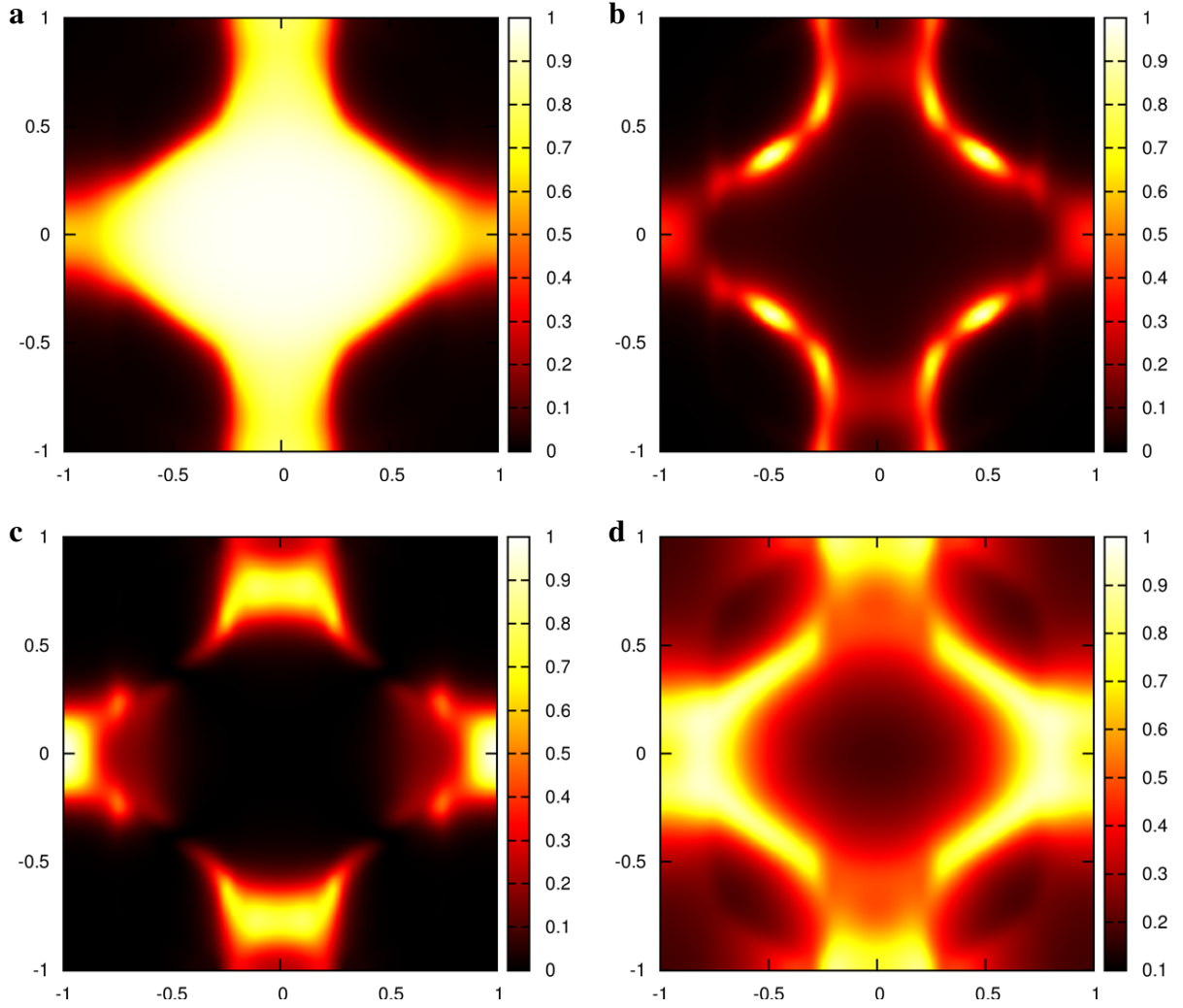
Figure 2. Momentum-space quantities of the striped phase of a clean d-wave superconductor. (a) Momentum distribution $n(\mathbf{k})$, (b) spectral density $A(\mathbf{k})$, (c) pair density $P(\mathbf{k})$ and (d) spin density $\rho_s(\mathbf{k})$ for $T = 0.025\,t$, $t' = -0.4\,t$, $V = 1.5\,t$, $x = 1/8$, $U = 3.3\,t$ and $V^{\mathrm{imp}} = 0$. Horizontal and vertical axes are given in units of π/a.

For a further characterization of the impurity-free case, we present in figure 2 momentum-space quantities. The momentum distribution $n(\mathbf{k})$ is shown in figure 2(a) and exhibits an anisotropy in k_x and k_y. In the presence of horizontal spin stripes, states with wave vectors near $\mathbf{k} \simeq (\pm\pi, 0)$ are less probably occupied than states near $\mathbf{k} \simeq (0, \pm\pi)$.

In a homogeneous d-wave superconductor, the spectral (quasi-particle) density $A(\mathbf{k})$ is finite only at the four points in the Brillouin zone where the SC order parameter has nodes. In the striped superconductor, it was shown that CDW order leads to an increase of spectral weight in the nodal direction, while SDW order suppresses spectral weight in this region [70]. Here we observe that spectral weight reappears on most of the Fermi surface of the normal conducting state (figure 2(b)). In the near nodal direction two peaks appear, which are fingerprints of both CDW and SDW order with a dominance of the latter. Comparing with [70], one can attribute

the peak around $\mathbf{k} \simeq (0.25, 0.6)\pi$ in the first quadrant of the Brillouin zone to spin order, while the peak at $\mathbf{k} \simeq (0.5, 0.4)\pi$ results from the charge order. These features bear resemblance to angle-resolved photoemission spectroscopy (ARPES) data found in $La_{2-x-y}Nd_ySr_xCuO_4$ and LSCO by Zhou *et al* [71]. Figure 2(c) shows the pair density $P(\mathbf{k})$ that accentuates the states contributing to superconductivity. The maxima in $A(\mathbf{k})$ around $\mathbf{k} \simeq (0.5, 0.4)\pi$ which originate from the CDW order [70] correspond to a suppression of the pairing in figure 2(c). $P(\mathbf{k})$ is maximal around $\mathbf{k} \simeq (\pm\pi, 0)$ where the pairing amplitude is largest. These regions resemble those of a homogeneous dSC, but stretching out less far into the nodal direction. In contrast, $P(\mathbf{k})$ is strongly suppressed at wave vectors $\mathbf{k} \simeq (0, \pm\pi)$ where the spin density is strong and exhibits local maxima around $\mathbf{k} \simeq (0, \pm 3/4\pi)$. The unidirectional character of the SDW is clearly seen in $\rho_s(\mathbf{k})$ (see figure 2(d)), which relates to the large amplitude oscillations of the staggered magnetization in real space. $\rho_s(\mathbf{k})$ dominates regions in momentum-space, which $P(\mathbf{k})$ would occupy in a non-magnetic homogeneous dSC. It extends far along the Fermi arcs, crossing the nodal points. $\rho_s(\mathbf{k})$ has large intensities in the anti-nodal regions, i.e. it competes with superconductivity. Although maxima of $\rho_s(\mathbf{k})$ are clearly separated from those of the pair density $P(\mathbf{k})$, both quantities coexist in large parts of momentum space.

3.1.2. Impurity-pinned stripes. In the presence of a *single* strong impurity with potential strength $V^{imp} = 10\,t$, the stripes are pinned as is inferred from the order parameter pattern shown in figure 1(b), where the impurity is located at the center. Impurity-pinned stripe solutions are robust against a change of the initial conditions, in contrast to the impurity-free stripe solution (figure 1(a)). Thus, we expect fluctuating stripes in real materials to be pinned by impurities and to become static. Horizontally equationed stripes emerge as well in the magnetization and the electron density. The impurity pins a channel of reduced pairing amplitude (figure 1(b)), which minimizes the loss of pairing energy. On the other hand, inhomogeneities in the order parameter result in a charge density redistribution in the absence of particle–hole symmetry [59]. In fact, the channels of reduced pairing amplitude collect electrons, thereby shifting the electron density in these channels toward half-filling. This in turn favors the emergence of AF order in the regions of enhanced electron density. That is why the impurity pins one of the ridges of the staggered magnetization. Altogether, electron-rich stripes coincide with strongly magnetized stripes of reduced pairing amplitude. The characteristics of the impurity-pinned stripes are similar to those of the impurity-free case, except that the impurity-pinned stripes emerge independently of the initial conditions. Thus the momentum-space quantities shown in figure 2 for the impurity-free stripe solution are essentially the same for the impurity-pinned stripes. Summarizing, we observe for sufficiently large on-site repulsion $U > U_c$, as in the impurity-free case, the coexistence of an mdSC, an SDW and a CDW with wavelength $\lambda_{CDW} = \lambda_{mdSC} = 4a = 1/2\,\lambda_{SDW}$ pinned by a single non-magnetic impurity.

Real-space quantities of stripes pinned by a single strong non-magnetic impurity have already been investigated by Chen and Ting [72]. They obtained similar results for the U-model at $x = 15\%$ hole doping, which is assumed to be close to optimal doping. We also checked that the periodicity of the stripes for a single impurity at $x = 1/10$ remains the same as for $x = 1/8$.

3.1.3. Vortex-pinned stripes. The vortex-pinned stripes shown in figure 3 display essentially the same properties as those for the impurity-free and the impurity-pinned stripes. The amplitudes of the mdSC, CDW and the SDW are marginally enhanced as compared to the impurity-pinned stripes, because a vortex penetrating the superconductor acts as a far stronger
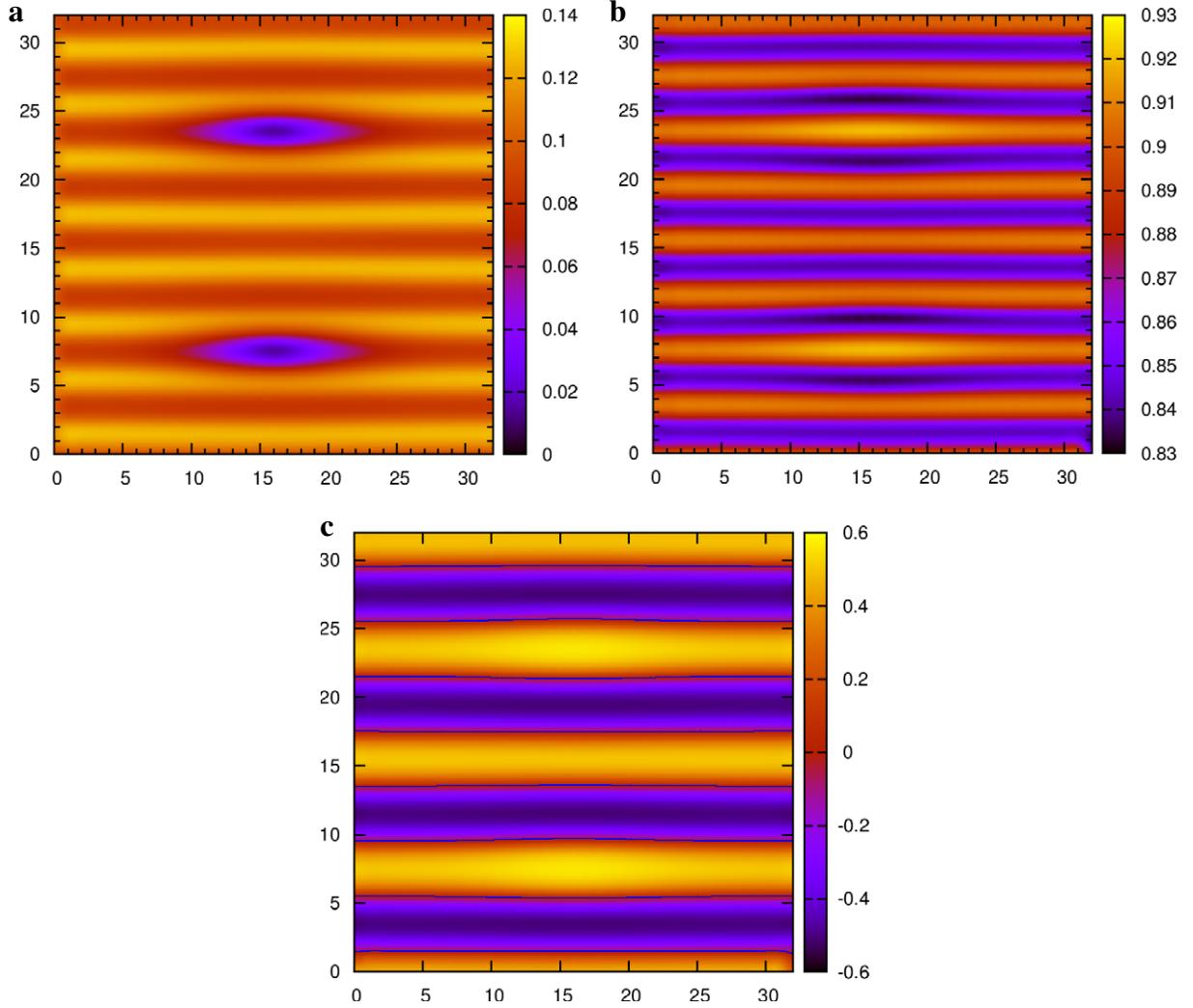
Figure 3. Vortex-pinned stripes. Results are shown for a magnetic flux $\Phi = 2\Phi_0$ penetrating a $32a \times 32a$ lattice which corresponds to a magnetic field $B = 25.6\,\mathrm{T}$. (a) SC order parameter, (b) electron density and (c) staggered magnetization (blue lines mark the zero-crossing). The model parameters were set to $T = 0.025\,t$, $t' = -0.4\,t$, $V = 1.34\,t$, $x = 1/8$, $U = 3.2\,t$.

perturbation than a single point-like impurity. Just like the impurity, the vortices pin the ridges of the SDW. Stripes of reduced pairing run through the elliptically deformed vortices and thereby save condensation energy. The AF stripes are further attracted by the vortex since vortex cores in d-wave superconductors strongly magnetize due to a spin-dependent splitting of the Andreev bound state [39, 59]. Correspondingly, the vortex pins an electron-rich stripe with a filling shifted toward 1/2. From the Fourier transforms of the real-space quantities, we obtain the same wavelength of the mdSC ($\lambda_{\mathrm{mdSC}} = 4a$), the CDW ($\lambda_{\mathrm{CDW}} = 4a$) and the SDW ($\lambda_{\mathrm{SDW}} = 8a$) at $x = 1/10$ and $1/8$. Similar results for coexisting CDWs and SDWs were observed in [63] within the U-model for vortex-pinned stripes above a critical U at $x = 15\%$ hole doping. Hence the wavelengths of these unidirectional density waves are identical in the impurity-free and

the impurity- and vortex-pinned stripes and robust against a change of hole doping or pairing interaction strength, as we verified by explicit calculations.

3.1.4. Disorder-pinned stripes. For the modeling of cuprates, such as BSCCO or those based on the parent compound La_2CuO_4, their dopant disorder has to be taken into account. In the following, we consider explicitly intrinsic disorder and compare our results with experimental data in zero and finite magnetic field. For modeling dopant disorder, we use randomly placed impurities with equal potentials V^{imp} and set the impurity concentration equal to the hole doping $n^{imp} = x$. Moreover, we assume that the dopants' impurity potential decreases with increasing hole doping due to enhanced screening [38]. Here we employ $V^{imp} = 1.3t$ for $x = 1/10$ and $V^{imp} = 0.9t$ for $x = 1/8$. In figures 4 and 5, we show exemplary results for two specific impurity configurations, which exhibit the characteristic behavior of the disordered stripe phase. We have verified that other impurity configurations yield density waves with the same wavelength as discussed here. For a Coloumb repulsion $U = 3.3t$ we find quasi-unidirectional stripes at $x = 1/8$, slightly deformed by the presence of the non-magnetic impurities (see figures 4(d)–(f)). Hole-rich paths (see figure 4(e)) coincide with anti-phase domain walls, seen in the staggered magnetization profile in figure 4(f), and with stripes of strong superconductivity as observed in the SC order parameter, figure 4(d). Although the suppression of the electron density on the impurity sites dominates the charge pattern as seen in figure 4(e), closer inspection reveals the existence of hole-rich channels (colored orange in figure 4(e)), where $\langle n_i \rangle$ is reduced compared to the average electron density. Additionally, the lines of zero staggered magnetization (blue lines in figure 4(f)), which coincide with the maxima of the SC order parameter, also serve as a guide to the eye. The d-wave order parameter (figure 4(d)) varies in the strong-disorder limit with much larger amplitudes as compared to the previous cases, but it never changes sign.

From the analysis of different disorder configurations, we conclude that the hole-rich paths emerge only close to $x = 1/8$ hole doping and sharpen upon approaching $x = 1/8$. Simultaneously, the density modulations as a whole become quasi-unidirectional. We find that, by shifting the hole doping toward 1/8, the system is driven into the stripe state. Moreover, we observe that the wavelength of the density modulation decreases by enhancing hole doping from $x = 1/10$ to 1/8 (cf figure 5). This characteristic, which is also observed in neutron-scattering experiments [73, 74], is not found in the impurity-free systems. Experimentally, SDWs with wavelengths $\lambda_{SDW}(x = 1/10) = 10a$ and $\lambda_{SDW}(x = 1/8) = 8a$ were inferred from the incommensurabilities. While this model calculation predicts exactly the same wavelength for the SDW at $x = 1/8$, the wavelength at $x = 1/10$ is slightly larger, that is $\lambda_{SDW} = 12a$, than in the experiment. Note that a decrease in hole density either reduces the amplitudes of the density waves or enhances the wavelength. The latter is valid in this model calculation. Strongly disordered systems support the former, where the random impurity sites facilitate the setup of additional hole channels. Disorder allows the stripe pattern to adjust more easily to the average hole density, whereas in the clean case, the stripe pattern is tied to the underlying lattice.

All real-space quantities verify horizontally (or vertically) oriented stripes at $x = 1/8$. The periodicity of these patterns is extracted from the FT quantities as shown in figure 5. Intriguingly, the FT data in the strong disorder regime for $x = 1/8$ (figures 5(d)–(f)) peak, in general, at the same wave vectors as for the perfectly unidirectional stripes discussed for clean systems. The magnetic structure factor (figure 5(f)) shows two dominating peaks at the incommensurate wave vectors $\mathbf{q}_m = \frac{2\pi}{a}(1/2, 1/2 \pm \epsilon)$ with incommensurability $\epsilon = 1/8$. The FT electron density (figure 5(e)) and the FT SC order parameter (figure 5(d)) exhibit similar
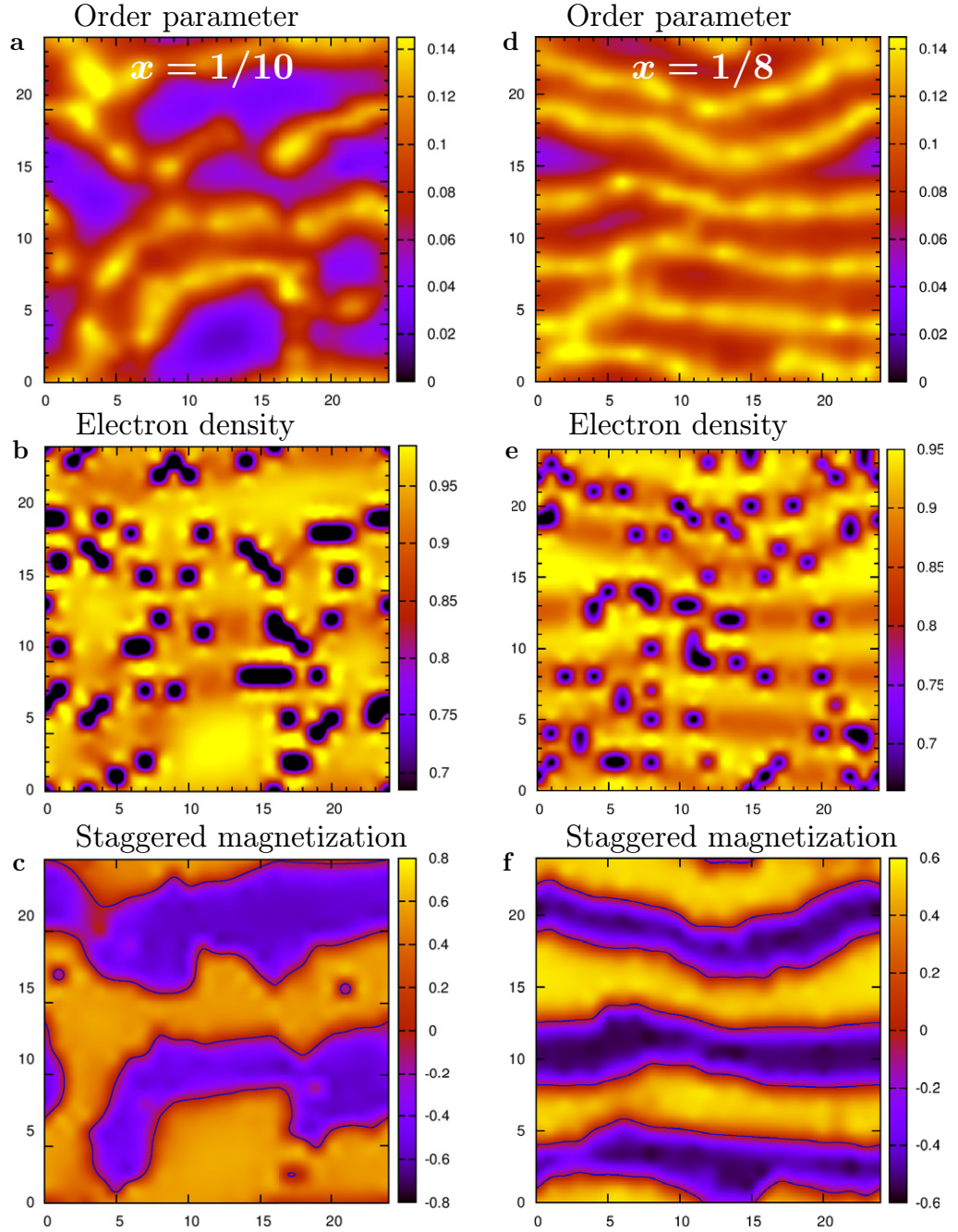
Figure 4. Emergence and stabilization of stripes in real-space quantities of d-wave superconductors by a shift of hole doping from 1/10 to 1/8 ($n_{\mathrm{imp}} = x$, $U = 3.3\,t$). For this set of parameters density modulations emerge close to $x = 1/10$ doping ($V^{\mathrm{imp}} = 1.3t$) in the presence of strong dopant disorder and become unidirectional by a change of hole doping toward 1/8 ($V^{\mathrm{imp}} = 0.9t$). (a), (d) SC order parameter Δ_i^{d}, (b), (e) electron density, (c), (f) staggered magnetization (blue lines mark the zero-crossing) for $T = 0.025\,t$, $t' = -0.4\,t$, $V = 1.6\,t$.
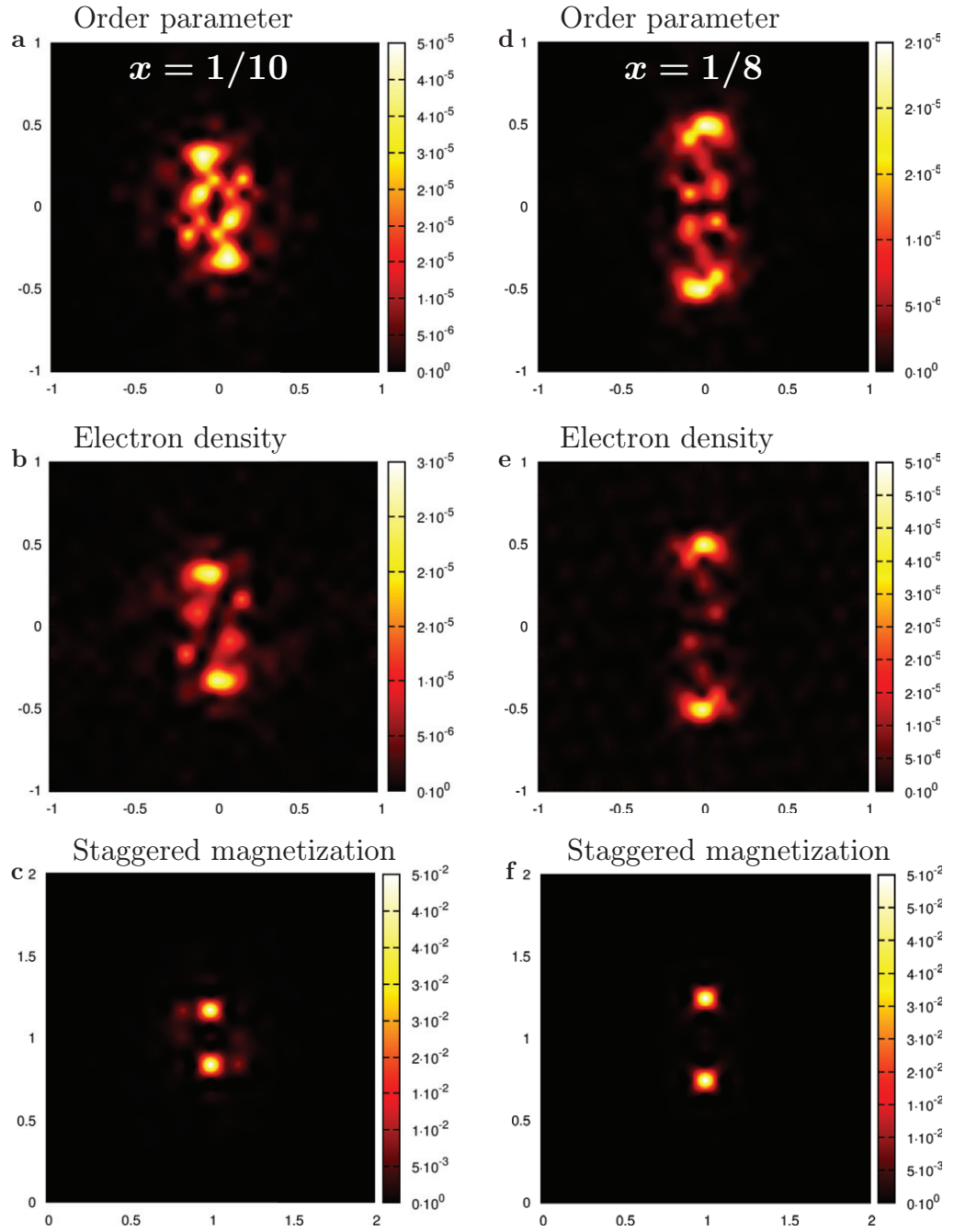
Figure 5. FT SC order parameter (a), (c), electron density (b), (e) and magnetic structure factor (c), (f) for 1/10 (a)–(c) and 1/8 (d)–(f) hole doping. The dopants' impurity potential is $V_{imp} = 0.9\,t$ at $x = 1/8$ and $V_{imp} = 1.3\,t$ at $x = 1/10$. Note that the impurity sites are not considered in the FT electron density (b), (e) as described in section 2.3. Parameters were fixed to $n_{dop} = x$, $U = 3.3\,t$, $T = 0.025\,t$, $t' = -0.4\,t$, $V = 1.6\,t$. Horizontal and vertical axes are given in units of π/a.

patterns with two broad maxima around wave vectors $\mathbf{q}_{c/p} \simeq 2\pi/a \, (0, \pm\delta)$ with $\delta = 1/4$. The main difference to the clean stripe solutions is that the peaks in figures 5(d) and (e) are broadened and a low-intensity substructure is observable. Obviously, the slight deviation from the characteristics of perfect unidirectional stripes is caused by the finite impurity concentration. While the correlation length of both charge and spin order is larger than the system size used, the spin-correlation length is even larger than the charge-correlation length (cf figures 5(e) and (f)). This agrees well with neutron scattering data obtained for LBCO [8].

We infer that coexisting mdSC, CDW and SDW with wavelength $\lambda_{mdSC} = \lambda_{CDW} = 4a$ and $\lambda_{SDW} = 8a$ persist at $x = 1/8$ even in the regime of strong disorder. The wavelengths of the density modulations change with doping as is recognized by comparison of 1/10 and 1/8 hole doping. In figures 5(a)–(c), the FT SC order parameter, the FT electron density and the magnetic structure factor are displayed for $x = 1/10$. The maxima deviate clearly from those at $x = 1/8$. At $x = 1/10$ the density modulations oscillate with wavelengths $\lambda_{SDW} \simeq 12a$ and $\lambda_{mdSC} \simeq 6a = \lambda_{CDW}$. In contrast to *weakly* disordered systems the incommensurabilities ϵ and δ in the strong disorder limit are sensitive to doping and increase with growing hole concentration.

The momentum-space quantities $n(\mathbf{k})$, $A(\mathbf{k})$, $P(\mathbf{k})$ and $\rho_s(\mathbf{k})$ (see figure 6) in the strong disorder limit resemble the results obtained for the impurity-free stripe solutions (see figure 2). Disorder slightly enhances the anisotropy, best visible in $\rho_s(\mathbf{k})$. Importantly, in the disordered system continuous Fermi arcs appear in the near nodal direction (see figure 6(b)). This agrees with ARPES measurements in LBCO [75], which has a strong dopant disorder. Oweing to the impurity potentials, through which the hole channels run, the CDW is stronger here as compared to the previously discussed cases, which results in the redistribution of spectral weight to the nodal directions [70].

Altogether, we find that an SDW, a CDW and an mdSC coexist at $x = 1/8$ hole doping in strongly disordered systems, such as dopant-disordered LSCO. The density modulations are pinned and stabilized, just as for a single impurity or a vortex, yet slightly deformed by the strong disorder. The doping dependence of the incommensurabilities $\epsilon \propto x$ and $\delta \propto x$ is similar to those observed in experiments [73, 74].

3.1.5. Density of states.   Characteristically, all the identified stripe solutions exhibit a full gap in the density of states (DOS) (see figure 7). For comparison also the typical v-shaped gap of a homogeneous d-wave superconductor is shown in figure 7. In the presence of stripes a full gap opens around the Fermi energy. The full gap is a generic property of stripes in d-wave superconductors , which persists also in the strong disorder limit. The full gap originates from a finite extended s-wave contribution in the striped d-wave superconductor and the SDW gap present in the strongly magnetized stripes. In a homogeneous d-wave superconductor, the bond order parameter Δ_{ij} changes sign between horizontal and vertical bonds which reflects the d-wave symmetry of the energy gap $\Delta_{\mathbf{k}}$. Thus the summation of Δ_{ij} over the vertical *and* horizontal bonds connecting to a given lattice site gives zero in a homogeneous dSC. Owing to the strong anisotropy of the stripe solutions, however, this summation yields a finite value here, which characterizes extended s-wave superconductors. So far, no experimental data for the DOS in the SC state of cuprates exhibiting static stripe order are available. The existence of an extended s-wave order-parameter component in these systems therefore still awaits experimental confirmation.
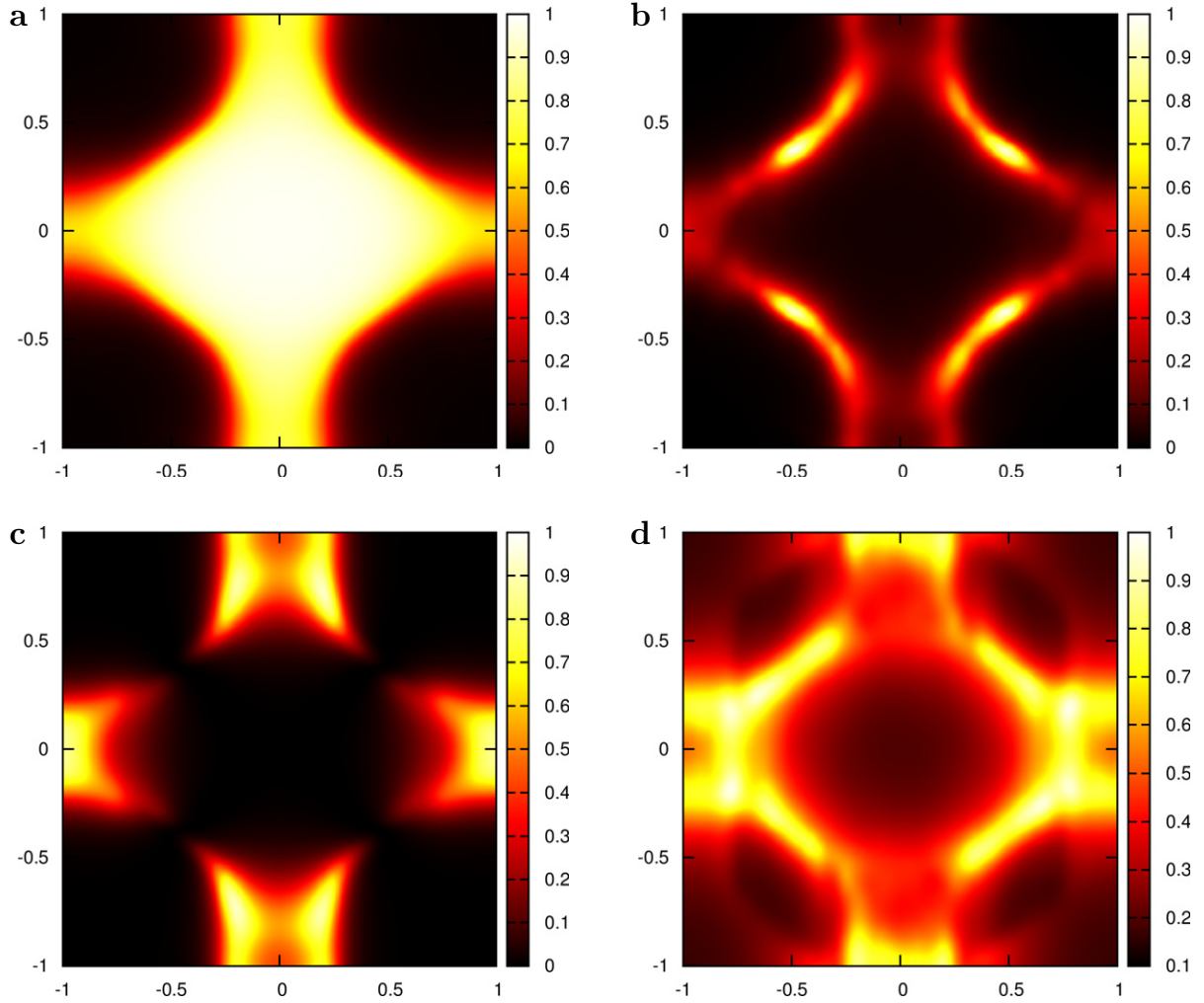
Figure 6. Momentum-space quantities in the strong disorder limit. (a) Momentum distribution $n(\mathbf{k})$, (b) spectral density $A(\mathbf{k})$, (c) pair density $P(\mathbf{k})$ and (d) spin density $\rho_s(\mathbf{k})$ for $T = 0.025\,t$, $t' = -0.4\,t$, $V = 1.6\,t$, $U = 3.3\,t$, $x = 1/8 = n_{\text{dop}}$, $V^{\text{dop}} = 0.9\,t$. Horizontal and vertical axes are given in units of π/a.

In a dSC coexisting with a SDW, the gap is generically not centered around the Fermi energy, which is the reason why the full gap is asymmetric in all stripe solutions shown in figure 7. In addition, particle–hole symmetry is already broken by the constant random impurity potentials with $V_{\text{imp}} > 0$. Experimentally, particle–hole anisotropy was observed recently by ARPES in the pseudogap phase of Bi-2201 [6], which is attributed to competing orders and contrasted to homogeneous superconductivity. The appearance of a full gap was also found by Loder *et al* [43]. Obviously, the gap is largest in the unperturbed stripe solution ($B = 0$, $V_{\text{imp}} = 0$). This is because with the impurity- and field-induced bound states, spectral weight is shifted into the energy gap.
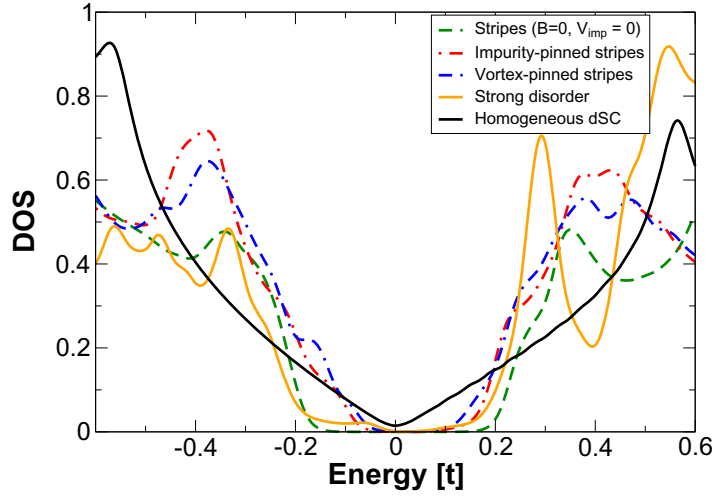
Figure 7. DOS in d-wave superconductors in the presence of stripes. Results for the data sets used above for impurity-free, impurity-pinned, vortex-pinned and disorder-stabilized stripe solutions for $x = 1/8$. The black curve corresponds to the DOS of a homogeneous d-wave superconductor.

3.2. Impurities in the V-model

The V-model presented by the Hamiltonian equation (6) was introduced in [43] as an alternative description for the coexistence of superconductivity with magnetic order. In the homogeneous case, the ground-state solution of the V-model for $x = 1/8$ is a mdSC state similar to figures 1(a, c). The main difference is that the AF stripes are nearly maximally magnetized, i.e. the SDW oscillates with an amplitude $\approx \mu_B$, while Δ_i^d goes to zero at the center of the AF stripes without changing sign. Thus magnetic order is dominating in the V-model, whereas superconductivity is reduced to straight, quasi-1D lines on the domain walls between the AF stripes. This mdSC solution is degenerate with a 'pure' PDW, which features a periodic sign change in Δ_i^d. Both, the 'pure' PDW and the mdSC have identical pair densities $P^2(\mathbf{k})$ (cf [43]).

In the strong disorder limit, the U- and the V-model show a severely different behavior. The solutions of the V-model can be divided into two regimes. If the scattering strength V^{imp} of the impurities is weak (i.e. $V^{imp} \lesssim t$), the AF stripes remain straight, as shown in figure 8. The magnetic energy gain is dominant and prevents the SC stripes to wind around the impurities, which would allow us to gain further condensation energy. Moreover, impurities in the straight 1D SC channels strongly suppress superconductivity. This effect culminates in the disappearance of the entire SC stripes, if the impurity density in their near vicinity becomes too large (figure 8(a)). One of the neighboring AF domains (see figure 8(c)) spreads over such a metallic line expelling the holes, which collect in the remaining SC stripes (figure 8(b)). In this situation, the AF domain-wall boundaries are shifted locally, according to the impurities' positions, but the AF spin stripes remain largely straight (figure 8(c)). The AF stripes are almost half-filled and all sites within the AF stripes are nearly fully polarized, in contrast to the small amplitude modulations seen in figure 4 for the U-model. Thus the SC stripes in the disordered V-model have a filling below 1/4 because the holes collect mainly in the remaining SC stripes. Similar to the SDW, also the CDW in the V-model modulates with much larger amplitudes as compared to the U-model.
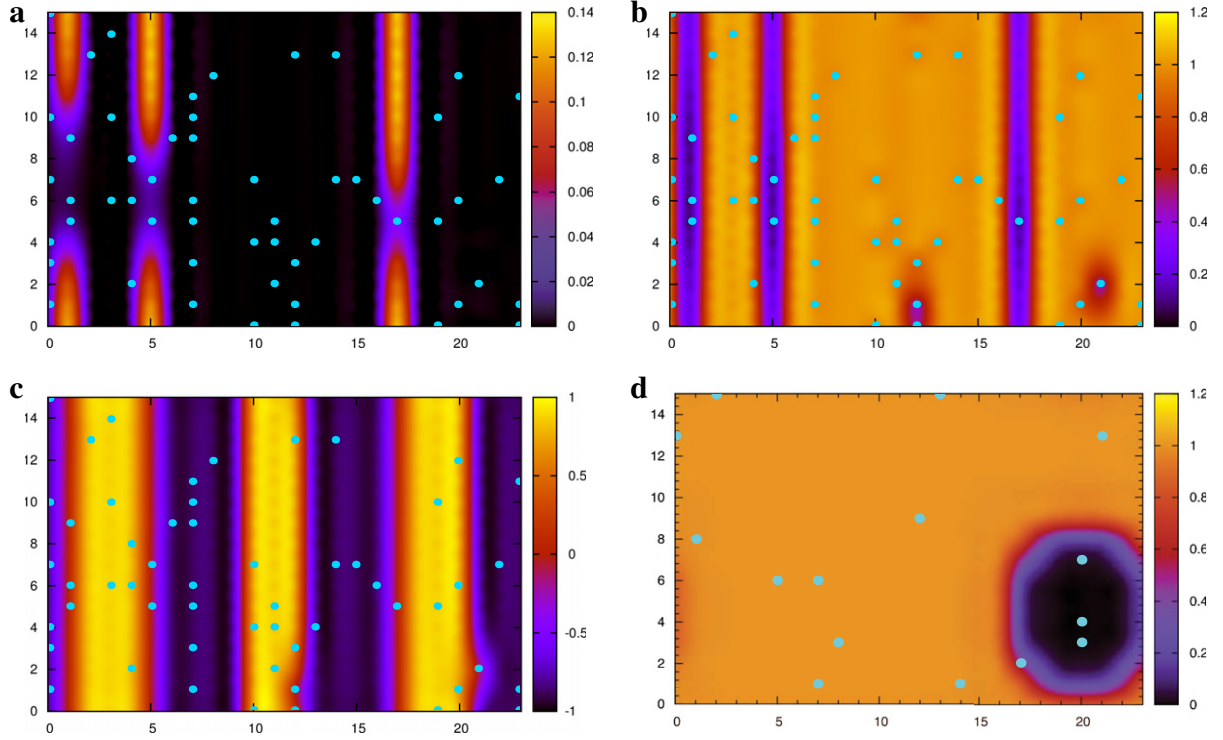
Figure 8. Stripe patterns in the disordered V-model. (a)–(c) Weak impurity potentials $V^{imp} = 0.9t$ $(x = 1/8 = n_{dop})$ and (d) strong impurity potentials $V^{imp} = 2.0t$ $(n_{dop} = 4\%)$. (a) Δ_i^d is d-wave order parameter. (b) Electron density. (c) Staggered magnetization. (d) Electron density exhibiting global phase separation for strong impurity potentials. The turquoise dots indicate the positions of the impurities. Parameters were fixed to $T = 0.01\,t$, $t' = -0.4\,t$, $V = 1\,t$.

If the impurity potentials V^{imp} become larger than t, we expect that the impurity-pinning of stripes is energetically favorable as long as a mdSC state prevails, similar to the U-model (cf figures 4(a)–(c)). However, we observe an overall disappearance of superconductivity accompanied by a global phase separation. All holes accumulate where the impurity concentration is the largest and antiferromagnetism is the weakest, while the surrounding region turns into a half-filled AF insulator (figure 8(d)). The same occurs if weak impurities are numerous enough to destroy sufficiently many metallic (SC) lines so that the remaining ones cannot accommodate all the holes in the system. This behavior is a characteristic for the strong-coupling limit described by the V-model: if the effectively 1D striped system is forced to become two dimensional because of the disorder, the system divides into half-filled and empty regions featuring global phase separation.

3.3. Discussion of the experimental observations in different cuprates

We found that the U-model allows for two-dimensional superconductivity in coexistence with a stripe order that adapts flexibly to disorder, while the solutions of the V-model remain quasi-1D. Materials in which three-dimensional superconductivity coexists with stripe order,

such as LBCO [7] or the rare-earth-doped cuprate $La_{2-x-y}Nd_ySr_xCuO_4$ with $x \lesssim 0.12$ and $y = 0.2$ [1, 12], are certainly not as 1D as the solution of the V-model. On the other hand the V-model reproduces the quasi-1D characteristics of Nd-doped LSCO around $y = 0.4$, quite well [43], where the material becomes more anisotropic with increasing doping. As argued in [44], the models described by $\mathcal{H}_U$ and $\mathcal{H}_V$ are the weak and strong coupling limits of a t–J-like model, and the cuprates are most likely found somewhere in the intermediate-coupling regime. This regime is not directly accessible within the mean-field evaluation used here. But the comparisons of the weak- and strong-coupling limits to experimental results give valuable insights.

The static, unidirectional CDWs and SDWs observed in LBCO and LNSCO [4] are often ascribed to the structural phase transition toward the LTT phase, where the LTT-specific buckling pattern of the CuO_6 octahedra induces an x–y anisotropy [76]. Our results imply that the strong dopant disorder, which is present in these substances, further stabilizes the stripe state. The results within the U-model in the strong disorder limit reproduce typical properties of these substances well, such as the Fermi arc reconstruction in LBCO [75] or LSCO [77] and the doping dependence of the wavelength of the SDW as inferred from neutron scattering experiments in LSCO [73, 74].

Although spin stripes are observed in LSCO at $x = 1/8$, an ordering of the charges has so far *not* been detected by neutron-scattering experiments [18, 19]. As LSCO does not exhibit an LTT phase we suggest that the experimentally observed spin stripes [18] are induced by the dopant disorder. The expected concomitant charge stripes are not found by neutron-scattering experiments possibly because the charge modulations are weak and may therefore be concealed by the reduction of the electron density below the dopant sites.

YBCO, which has neither an effective dopant disorder nor a LTT phase, exhibits dynamic instead of static stripes [20, 78]. This agrees with the results of the U-model for an impurity-free system as discussed. In the presence of a magnetic field charge stripes become static, while spin stripes are absent [23]. In this case, the magnetic field weakens superconductivity, allowing charge stripes to emerge. We find a similar behavior in the U-model when we turn off superconductivity deliberately. The magnetization is greatly suppressed, while a dominant charge order survives.

4. Summary

The models we investigated in this paper allow us to explain a wide range of features of striped cuprate superconductors, which were found experimentally. Notably, the material-specific characteristics of stripe phases in various cuprates can be modelled within the U-model. On the other hand, we found that AF correlations in the V-model tend to be stronger and the SC stripes are 1D, which reproduces some characteristics of Nd-doped LSCO quite well.

Specifically, we found the coexistence of PDW's, SDW's and CDW's with wavelengths $\lambda_{CDW} = \lambda_{PDW} = 4a = 1/2\,\lambda_{SDW}$ in a d-wave superconductor for sufficiently large U in the U-model. Impurity-free, (single) impurity-pinned and vortex-pinned *straight* stripe solutions exist over a broad doping range in the U-model. Disorder dissolves the strict 1D stripe order into meandering stripe-like patterns. Only close to $x = 1/8$ hole doping, which is ideal for stripe formation, a unidirectional stripe order reemerges in strongly disordered systems. Since in clean systems, the stripe pattern remains unchanged over a broad range of hole concentrations,

IOP Institute of Physics ⦿ DEUTSCHE PHYSIKALISCHE GESELLSCHAFT

disorder appears to be essential in understanding the flexible adaption of the stripe wavelength to variations of hole doping as observed experimentally.

In the V-model, stripes are rigid and remain 1D and virtually undistorted in the presence of weak disorder. Although SC stripes react sensitively to disorder and may even be removed in particular SC channels, the stripe pattern and its wavelength do not adapt to impurities or a change of the hole concentration. Strong disorder, however, leads to global phase separation into dominantly AF regions with non-magnetic puddles absorbing the holes. The disordered U-model is therefore best suited for describing the physics of most cuprate materials which display a stripe phase.

The overall identical characteristics of the impurity-, vortex-pinned and (strong) disorder-pinned stripes indicate that the stripes are not generated by impurities or fields. Instead, stripe states, which are energetically close to homogeneous solutions in unperturbed systems, are pinned and stabilized by inhomogeneities which are connected to charge redistributions.

A generic feature of striped d-wave superconductors in both the U- and the V-model is the opening of a full gap, induced by an extended s-wave contribution. Without local probes for the SC order parameter it is not clear if pair-density modulations accompany the charge- and spin stripe order.

Acknowledgment

References

[1] Tranquada J M, Sternlieb B J, Axe J D, Nakamura Y and Uchida S 1995 *Nature* **375** 561
[2] Kivelson S A, Bindloss I P, Fradkin E, Oganesyan V, Tranquada J M, Kapitulnik A and Howald C 2003 *Rev. Mod. Phys.* **75** 1201
[3] Tranquada J M, Woo H, Perring T G, Goka H, Gu G D, Xu G, Fujita M and Yamada K 2004 *Nature* **429** 534
[4] Fujita M, Goka H, Yamada K, Tranquada J M and Regnault L P 2004 *Phys. Rev.* B **70** 104517
[5] Komiya S, Ando Y, Sun X F and Lavrov A N 2002 *Phys. Rev.* B **65** 214535
[6] Hashimoto M, He R H, Tanaka K, Testaud J P and Meevasana W 2010 *Nature Phys.* **6** 414
[7] Hücker M, Zimmermann M V, Gu G D, Xu Z J, Wen J S, Xu G, Kang H J, Zheludev A and Tranquada J M 2011 *Phys. Rev.* B **83** 104506
[8] Tranquada J M *et al* 2008 *Phys. Rev.* B **78** 174529
[9] Dunsiger S R, Zhao Y, Yamani Z, Buyers W J L, Dabkowska H A and Gaulin B D 2008 *Phys. Rev.* B **77** 224410
[10] Abbamonte P, Rusydi A, Smadici S, Gu G D, Sawatzky G A and Feng D L 2005 *Nature Phys.* **1** 155
[11] Kim Y J, Gu G D, Gog T and Casa D 2008 *Phys. Rev.* B **77** 064520
[12] Büchner B, Breuer M, Freimuth A and Kampf A P 1994 *Phys. Rev. Lett.* **73** 1841
[13] Zimmermann M V *et al* 1998 *Europhys. Lett.* **41** 629
[14] Christensen N B, Rønnow H M, Mesot J, Ewings R A, Momono N, Oda M, Ido M, Enderle M, McMorrow D F and Boothroyd A T 2007 *Phys. Rev. Lett.* **98** 197003
[15] Li Q, Hücker M, Gu G D, Tsvelik A M and Tranquada J M 2007 *Phys. Rev. Lett.* **99** 067001
[16] Sawa T, Matsumura M and Yamagata H 2001 *J. Phys. Soc. Japan* **70** 3503
[17] Klauss H-H, Wagener W, Hillberg M, Kopmann W, Walf H, Litterst F J, Hücker M and Büchner B 2000 *Phys. Rev. Lett.* **85** 4590

[18] Suzuki T, Goto T, Chiba K, Shinoda T, Fukase T, Kimura H, Yamada K, Ohashi M and Yamaguchi Y 1998 *Phys. Rev.* B **57** R3229

[19] Kimura H *et al* 1999 *Phys. Rev.* B **59** 6517

[20] Vojta M 2010 *Eur. Phys. J. Spec. Top.* **188** 49

[21] Hinkov V, Haug D, Fauqué B, Bourges P, Sidis Y, Ivanov A, Bernhard C, Lin C T and Keimer B 2008 *Science* **319** 597

[22] Daou R *et al* 2010 *Nature* **463** 519

[23] Wu T, Mayaffre H, Krämer S, Horvatić M, Berthier C, Hardy W N, Liang R, Bonn D A and Julien M-H 2011 *Nature* **477** 191

[24] Zaanen J and Gunnarsson O 1989 *Phys. Rev.* B **40** 7391

[25] Vojta M and Ulbricht T 2004 *Phys. Rev. Lett.* **93** 127002

[26] Greiter M and Schmidt H 2010 *Phys. Rev.* B **82** 144512

[27] Machida K 1989 *Physica* C **158** 192

[28] Fleck M, Lichtenstein A I and Oleś A M 2001 *Phys. Rev.* B **64** 134528

[29] Tohyama T, Nagai S, Shibata Y and Maekawa S 1999 *Phys. Rev. Lett.* **82** 4910

[30] White S R and Scalapino D J 1998 *Phys. Rev. Lett.* **80** 1272

[31] White S R and Scalapino D J 1998 *Phys. Rev. Lett.* **81** 3227

[32] White S R and Scalapino D J 2000 *Phys. Rev.* B **61** 6320

[33] Martins G B, Gazza C, Xavier J C, Feiguin A and Dagotto E 2000 *Phys. Rev. Lett.* **84** 5844

[34] Hellberg C S and Manousakis E 1997 *Phys. Rev. Lett.* **78** 4609

[35] Hellberg C S and Manousakis E 2000 *Phys. Rev.* B **61** 11787

[36] Himeda A, Kato T and Ogata M 2002 *Phys. Rev. Lett.* **88** 117001

[37] Buhler C, Yunoki S and Moreo A 2000 *Phys. Rev. Lett.* **84** 2690

[38] Andersen B M, Hirschfeld P J, Kampf A P and Schmid M 2007 *Phys. Rev. Lett.* **99** 147002

[39] Schmid M, Andersen B M, Kampf A P and Hirschfeld P J 2010 *New J. Phys.* **12** 053043

[40] Andersen B M and Hedegård P 2005 *Phys. Rev. Lett.* **95** 037002

[41] Raczkowski M, Capello M, Poilblanc D, Frésard R and Oleś A M 2007 *Phys. Rev.* B **76** 140505

[42] Yang K-Y, Chen W Q, Rice T M, Sigrist M and Zhang F C 2009 *New J. Phys.* **11** 055053

[43] Loder F, Graser S, Kampf A P and Kopp T 2011 *Phys. Rev. Lett.* **107** 187001

[44] Loder F, Graser S, Schmid M, Kampf A P and Kopp T 2011 *New J. Phys.* **13** 113037

[45] Berg E, Fradkin E and Kivelson S A 2009 *Phys. Rev.* B **79** 064515

[46] Berg E, Fradkin E, Kivelson S A and Tranquada J M 2009 *New J. Phys.* **11** 115004

[47] Scalapino D J 1994 *Proc. Int. Summer School of Physics 'Enrico Fermi' (July 1992)* (Amsterdam: North-Holland) p 95

[48] MacDonald A H, Girvin S M and Yoshioka D 1988 *Phys. Rev.* B **37** 9753

[49] Kane C L, Lee P A and Read N 1989 *Phys. Rev.* B **39** 6880

[50] Jayaprakash C, Krishnamurthy H R and Sarker S 1989 *Phys. Rev.* B **40** 2610

[51] Fresard R and Wölfle P 1992 *J. Phys.: Condens. Matter* **4** 3625

[52] Yu M Kagan and Rice T M 1994 *J. Phys.: Condens. Matter* **6** 3771

[53] Lee P A, Nagaosa N, Ng T-K and Wen X-G 1998 *Phys. Rev.* B **57** 6003

[54] Chen Y and Ting C S 2004 *Phys. Rev. Lett.* **92** 077203

[55] Harter J W, Andersen B M, Bobroff J, Gabay M and Hirschfeld P J 2007 *Phys. Rev.* B **75** 054520

[56] Alloul H, Bobroff J, Gabay M and Hirschfeld P J 2009 *Rev. Mod. Phys.* **81** 45

[57] Andersen B M, Schmid M, Graser S, Hirschfeld P J and Kampf A P 2011 *J. Phys. Chem. Solids* **72** 358

[58] Zhu J X and Ting C S 2001 *Phys. Rev. Lett.* **87** 147002

[59] Schmid M 2011 *Disorder- and Field-Induced Inhomogeneities in Unconventional Superconductors* Dr Hut, Munich

[60] Agterberg D F and Tsunetsugu H 2008 *Nature Phys.* **4** 639

[61] Vojta M 2009 *Adv. Phys.* **58** 699

[62] Baruch S and Orgad D 2008 *Phys. Rev.* B **77** 174502
[63] Chen Y, Chen H Y and Ting C S 2002 *Phys. Rev.* B **66** 104501
[64] Tricoli U and Andersen B M 2012 *J. Supercond. Nov. Magn.* **25** 1329
[65] Zhu J X, Martin I and Bishop A R 2002 *Phys. Rev. Lett.* **89** 067003
[66] Andersen B M, Graser S and Hirschfeld P J 2010 *Phys. Rev. Lett.* **105** 147002
[67] Del A Maestro, Rosenow B and Sachdev S 2006 *Phys. Rev.* B **74** 024520
[68] Robertson J A, Kivelson S A, Fradkin E, Fang A C and Kapitulnik A 2006 *Phys. Rev.* B **74** 134507
[69] Loder F, Kampf A P and Kopp T 2010 *Phys. Rev.* B **81** 020511
[70] Jiang H-M, Chen C-P and Li J-X 2009 *J. Phys.: Condens. Matter* **21** 375701
[71] Zhou X J *et al* 2001 *Phys. Rev. Lett.* **86** 5578
[72] Chen H-Y and Ting C S 2003 *Phys. Rev.* B **68** 212502
[73] Yamada K, Lee C H, Kurahashi K, Wada J, Wakimoto S, Ueki S, Kimura H and Endoh Y 1998 *Phys. Rev.* B **57** 6165
[74] Fujita M, Yamada K, Hiraka H, Gehring P M, Lee S H, Wakimoto S and Shirane G 2002 *Phys. Rev.* B **65** 064505
[75] Valla T, Fedorov A V, Lee J, Davis J C and Gu G D 2006 *Science* **314** 1914
[76] Kampf A P, Scalapino D J and White S R 2001 *Phys. Rev.* B **64** 052509
[77] Razzoli E *et al* 2010 *New J. Phys.* **12** 125003
[78] Stock C, Buyers W J L, Liang R, Peets D, Tun Z, Bonn D, Hardy W N and Birgeneau R J 2004 *Phys. Rev.* B **69** 014502